Empirical social triad statistics can be explained with dyadic homophylic interactions

Tuan Minh Pham[a,b], Jan Korbel[a,b], Rudolf Hanel[a,b], and Stefan Thurner[a,b,c,1]

[a]Section for the Science of Complex Systems, Center for Medical Statistics, Informatics and Intelligent Systems, Medical University of Vienna, A-1090 Vienna, Austria; [b]Complexity Science Hub, A-1090 Vienna, Austria; and [c]Santa Fe Institute, Santa Fe, NM 87501

Edited by Christopher Jarzynski, Institute for Physical Science and Technology, Department of Chemistry and Biochemistry and Department of Physics, University of Maryland at College Park, College Park, MD; received November 24, 2021; accepted December 27, 2021

The remarkable robustness of many social systems has been associated with a peculiar triangular structure in the underlying social networks. Triples of people that have three positive relations (e.g., friendship) between each other are strongly overrepresented. Triples with two negative relations (e.g., enmity) and one positive relation are also overrepresented, and triples with one or three negative relations are drastically suppressed. For almost a century, the mechanism behind these very specific ("balanced") triad statistics remained elusive. Here, we propose a simple realistic adaptive network model, where agents tend to minimize social tension that arises from dyadic interactions. Both opinions of agents and their signed links (positive or negative relations) are updated in the dynamics. The key aspect of the model resides in the fact that agents only need information about their local neighbors in the network and do not require (often unrealistic) higher-order network information for their relation and opinion updates. We demonstrate the quality of the model on detailed temporal relation data of a society of thousands of players of a massive multiplayer online game where we can observe triangle formation directly. It not only successfully predicts the distribution of triangle types but also explains empirical group size distributions, which are essential for social cohesion. We discuss the details of the phase diagrams behind the model and their parameter dependence, and we comment on to what extent the results might apply universally in societies.

social balance | signed networks | social stability

Recognizing the fundamental role of triadic interactions in shaping social structures, Heider (1) introduced the notion of balanced and unbalanced triads. A triad (triangle) of individuals is balanced if it includes zero or two negative links; otherwise, it is unbalanced. Heider (1) hypothesized that social networks have a tendency to reduce the number of unbalanced triangles over time such that balanced triads would dominate in a stationary situation. This theory of "social balance" has been confirmed empirically in many different contexts, such as schools (2), monasteries (3), social media (4), or computer games (5). Social balance theory and its generalizations (6–8) have been studied extensively for more than a half century for their importance in understanding polarization of societies (9), global organization of social networks (10), evolution of the network of international relations (11), opinion formation (12, 13), epidemic spreading (14, 15), government formation (16), and decision-making processes (17).

Following Heider's intuition (18–41), current approaches toward social balance often account for the effect of triangles on social network formation in one way or another. For example, the models in refs. 22 and 23 consider a reduction of the number of unbalanced triads either in the neighborhood of a node or in the whole network. The latter process sometimes leads to imbalance due to the existence of so-called jammed states (42). In order to reach social balance, individuals can also update their links according to their relations to common neighbors (18–21) or adjust link weights via opinion updates (24, 25) or via a minimization of social stress based on triadic interactions (37–44). These works not only ignore the difficulty of individuals to know the social interactions beyond their direct neighbors in reality, so far, they also have not considered the detailed statistical properties of the over- or underrepresentation of the different types of triads, such as those reported in refs. 4 and 5, with the exception of refs. 43 and 44.

It is generally believed that the similarity of individuals plays a crucial role in the formation of social ties in social networks, something that has been called homophily (45–48). This means that to form a positive or negative tie with another person, people compare only pairwise overlaps in their individual opinions (dyadic interaction). It has also been argued that social link formation takes into account a tendency in people to balance their local interaction networks in the sense that they introduce friends to each other, that they do give up friendships if two mutual friends have negative attitudes toward each other, and that they tend to avoid situations where everyone feels negatively about the others. This is the essence of social balance theory (1). Obviously, link formation following social balance is cognitively much more challenging than homophily-based link formation since in the former, one has to keep in mind the many mutual relations between all your neighbors in a social network. While social balance–driven link formation certainly occurs in the context of close friendships, it is less realistic to assume that

Significance

Social stability is often associated with triangular interactions between people. Various possible social triangles appear in peculiar ratios. The triangles "The friend of my friend is my friend" and "The enemy of my friend is my enemy" are strongly overrepresented, which plays an important role for social balance. A standard explanation for these characteristic triangle fractions is that people consider triadic information before forming social relations. This assumption often contradicts everyday experience. We propose an explanation of the observed overrepresentations without individuals having to consider triangles. A society where individuals minimize their social stress self-organizes toward the empirically observed triangular structures. We demonstrate this with data from a society of computer game players, where triangle formation can be directly observed.

Author contributions: T.M.P. and S.T. designed research; T.M.P. and R.H. performed research; T.M.P., J.K., and S.T. analyzed data; and T.M.P. and S.T. wrote the paper.

The authors declare no competing interest.

This article is a PNAS Direct Submission.

[1]To whom correspondence may be addressed. Email: stefan.thurner@meduniwien.ac.at.

This article contains supporting information online at https://www.pnas.org/lookup/suppl/doi:10.1073/pnas.2121103119/-/DCSupplemental.

Published Febuary 1, 2022.

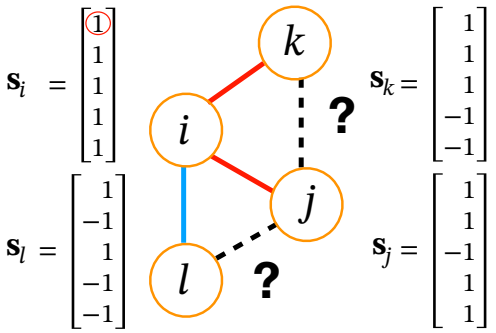

Fig. 1. Schematic view of opinion and link updates in a society. Every individual has an opinion vector whose components represent (binary) opinions on $G = 5$ different subjects. Red (blue) links denote positive (negative) relationships. The question marks denote unknown relationships between *i*'s neighbors. As an agent *i* flips one of its opinions (red circle), s_i^1, from 1 to -1, *i* can either decrease or increase its individual stress, $H^{(i)}$, depending on the value of the parameter α (Eq. **1**). For instance, $H^{(i)}$ would increase if $\alpha = 1$ but would decrease for $\alpha = 0$. For high "rationality" values of individuals w.r.t. social stress, as quantified by β, the latter is more likely to be accepted, resulting in a reduction of the number of unbalanced triads in *i*'s neighborhood.

this mechanism is at work in social link formation in general. In Fig. 1, we schematically show the situation in a portion of a social network. It is generally hard for node *i* to know all the relations between his neighbors *j*, *k*, and *l*.

Here, assuming that it is generally unrealistic for individuals to know their social networks at the triadic level, we aim to understand the emergence and the concrete statistics of balanced triads on the basis of dyadic or one-to-one interactions. Therefore, we use a classic homophily rule (45, 46) to define a "stress level" between any pair of individuals based on the similarity (or overlap) of their individual opinions. Here, the opinions of an individual *i* are represented by a vector with *G* components, $\mathbf{s}_i$, that we show in Fig. 1. Homophily implies that *i* and *j* tend to become friends if the overlap (e.g., scalar product of their opinion vectors) is positive, and they become enemies if the overlap is negative. Such a specification of homophily is often referred to as an attraction–repulsion or assimilation–differentiation rule (49, 50). Assuming that, generally, social relations rearrange such as to minimize individual social stress on average, we will show that balanced triads naturally emerge from purely dyadic homophilic interactions without any explicit selection mechanisms for specific triads. We formulate the opinion link dynamics leading to social balance within a transparent physics-inspired framework. In particular, we observe a dynamic transition between two different types of balanced steady states that correspond to different compositions of balanced triads.

Explaining the empirical statistics of triangles in social systems is a challenge. Early works considered groups of a few monks in a monastery (3) or a few students in classrooms (51). The studies suffered from limited data and small network sizes. Large-scale studies were first performed in online platforms (4) and in the society of players of the massive multiplayer online game (MMOG) *Pardus*. Players in *Pardus* engage in a form of economic life, such as trade and mining, and in social activities, such as communication on a number of channels, forming friendships and enmities (details are in refs. 5, 52, and 53). In the social networks of this game, balanced triads were once more confirmed to be overrepresented compared with what is expected by chance. Similar patterns of triad statistics were also observed in Epinion, Slashdot, and Wikipedia (4). More details on the *Pardus* society are in *Materials and Methods*. This dataset gives us the unique possibility to validate the model and compare the predictions with actual triangle statistics and formation of positively connected groups that are foundational to social cohesion.

Results

We implement a simple model that updates signed links (positive for friendship, negative for enmity) and opinions of individuals according to a stress-minimization scheme. We consider a social network with *N* nodes that represent individuals. Links represent their social relationships. Every individual *i* is linked to k_i others and holds binary opinions on $G > 1$ issues, $\mathbf{s}_i \in \{-1, 1\}^G$ (i.e., $\mathbf{s}_i$ is a *G*-dimensional vector, its entries being binary opinions). If two individuals *i* and *j* are connected by a link J_{ij}, its sign is determined by the similarity between the respective opinions: $J_{ij} = \text{sign}(\mathbf{s}_i \cdot \mathbf{s}_j)$, similar to what was done in ref. 24. $J_{ij} = -1$ denotes enmity, and $J_{ij} = 1$ is friendship. Note that with this definition, for $G = 1$, we have $J_{ij}J_{jk}J_{ki} = (s_i s_j)(s_j s_k)(s_k s_i) = 1$, $\forall\,(i, j, k)$. This means that, trivially, all triads are balanced for $G = 1$, regardless of the individuals' opinions. Therefore, we do not consider the case of $G = 1$ in our model. Moreover, since for an even number of *G*, there can be a "tie" (an equal number of similar and dissimilar attributes between *i* and *j*), we only consider odd *G* values. Every individual, *i*, has a local social stress function defined as

$$H^{(i)} = -\frac{\alpha}{G}\sum_{j:J_{ij}=1}\mathbf{s}_i\cdot\mathbf{s}_j + \frac{1-\alpha}{G}\sum_{j:J_{ij}=-1}\mathbf{s}_i\cdot\mathbf{s}_j, \qquad [1]$$

where the first sum includes all friends of *i* and the second includes all enemies. The parameter $\alpha \in [0, 1]$ controls the relative weight of these terms. For a positive link, its relative weight is α/G, and for a negative link, it is $(\alpha - 1)/G$. The intuition behind this is that one tries to harmonize relations within the friend group and be on unfriendly terms in the other group. Note that a global Hamiltonian $E = \sum_i H^{(i)}$ for $\alpha = 0.5$ and $G = 1$ was studied in refs. 10 and 35. The dynamics that we implement in the following, however, only complies with our choice of $G > 1$. For $G = 1$, there is no genuine disorder in the model as any negative coupling $J_{ij} = \text{sign}\left(s_i s_j\right) = -1$ can be removed by a gauge transformation (54) of the form $s_i \to \tilde{s}_i = \tau_i s_i$, $s_j \to \tilde{s}_j = \tau_j s_j$, with $\tau_i, \tau_j \in \{-1, 1\}$ and $\tau_i\tau_j = -1$ so that $\tilde{J}_{ij} := \text{sign}\left(\tilde{s}_i\tilde{s}_j\right) = \text{sign}\left(\tau_i\tau_j s_i s_j\right) = 1$ (for a positive coupling, instead we need to choose a pair of τ_i and τ_j such that $\tau_i\tau_j = 1$, and hence, $\tilde{J}_{ij}$ is also equal to 1). In terms of the new variables, $\tilde{s}_i$, the local stress becomes $H^{(i)} = -\alpha\sum_j \tilde{s}_i\tilde{s}_j$ (i.e., it reduces to the energy of the Ising model) (55). Assuming that agents tend to minimize their individual stress over time, the dynamics includes three steps.

1) Initialization. Every node is assigned an opinion vector, $\mathbf{s}_i$, whose components are randomly chosen to be 1 or -1 with equal probability. The network topology is fixed (who knows whom). In the simplest version, we chose a fixed ring topology, where every node *i* is connected with exactly $k_i = K$ nearest neighbors. For any pair of neighbors, *i* and *j*, we set $J_{ij} = \text{sign}(\mathbf{s}_i \cdot \mathbf{s}_j)$.
2) Update.
   (i) Pick a node *i* randomly, and compute $H^{(i)}$ in the current state. Its value is $\mathcal{H}$.
   (ii) Flip one of *i*'s opinion attributes at random. The new opinion of *i* is $\tilde{\mathbf{s}}_i$. Compute the new stress $\tilde{\mathcal{H}}$, and $\Delta H^{(i)} \equiv \tilde{\mathcal{H}} - \mathcal{H}$.
   (iii) Update $\mathbf{s}_i \to \tilde{\mathbf{s}}_i$ and $J_{ij} \to \tilde{J}_{ij} = \text{sign}(\tilde{\mathbf{s}}_i \cdot \mathbf{s}_j)$ with probability $\min\left\{e^{-\beta\Delta H^{(i)}}, 1\right\}$, where β is a constant explained below; otherwise, leave it unchanged.
3) Continue with the next opinion and link updates by returning to step 2.

The relevant parameters of the model are, therefore, the relative weights for the friend and enemy groups α, the rationality of individuals with respect to (w.r.t.) social stress (inverse temperature) β, the network topology, and the degree sequence of the nodes $\{k_i\}$. More details and a discussion of model variants are in *SI Appendix*, section A. Note that contrary to the $G = 1$ case (*SI Appendix*, section L), with randomized opinions in the initial configuration, we always approximately get the same number of balanced and unbalanced triangles for sufficiently large values of G.

Emergence of Social Balance from Dyadic Interactions. Let n_+ and n_- be the numbers of balanced and unbalanced triads, respectively. Following Heider's triad-based definition of balance, we quantify the level of social balance by an order parameter given by the relative difference of balanced and unbalanced triangles, $f = (n_+ - n_-)/(n_+ + n_-)$. The balanced state ($n_- = 0$) corresponds to $f = 1$, and the unbalanced corresponds to $f \simeq 0$ since $n_+ \simeq n_-$. In contrast to refs. 7, 56, and 57, we do not use motives larger than triangles since they seem to have less sociological justification (58). Apart from f, we further consider other measures that exist in any kind of graph topology (including graphs without triangles). In particular, we calculate the global social stress, $E = \sum_i H^{(i)}$, and the average similarity score, C; Eq. **3** in *Materials and Methods* shows its definition. While E can be used to characterize the overall stress landscape of the society, C acts as a local measure of how much, on average, an individual agent agrees with its friends. Finally, one might be interested in quantifying the level of "weak" balance (8), where $(---)$ triads are also considered as balanced. As seen below, this kind of triad is present with a marginal number in both balanced and unbalanced regions in the phase diagram, making the reported phase transition compatible with the concept of weak balance.

For a wide range of parameters, we find the emergence of social balance in the steady state (*SI Appendix*, section K has a detailed time series of all the measures). In Fig. 2, there exists a balanced phase ($f \sim 1$; yellow) in the phase diagrams for societies with $G = 9$ (Fig. 2*A*) and $G = 27$ (Fig. 2*B*) opinions on a regular network with a ring topology. For any fixed value of α, a transition from an unbalanced to a balanced phase occurs where $f \simeq 0.1 \rightarrow \sim 1$, as inverse temperature, β, increases. We find that the critical β_c, at which the transition happens, depends on the number of opinions, G, and the average degree, K, in a power law fashion, $\beta_c \propto G^{\gamma} K^{-\gamma'}$. Note that $\gamma(\alpha)$ increases as α increases from 0 to 0.5 and then, drops as α goes from 0.5 to 1. We observe that β_c is finite, and β_c decreases with increasing K. Details on the critical behavior and the robustness of the transition with respect to changing system size, N, are in *SI Appendix*, sections B and C. The balanced–unbalanced phase transition also exists on different network topologies, such as small world (59) (*SI Appendix*, section A) or a realistic social network with the same topology as that of the *Pardus* network (see Fig. 5*A*). In all cases, we observe a phase diagram similar to Fig. 2*A* but with a smaller critical value β_c than that of ring networks with the same average degree and $G = 9$ fixed. This suggests that societies with a more heterogeneous topology are more likely to become balanced at relatively high temperature than societies with a regular pattern of connectivities. We show that, as β increases, both measures, E and C, undergo similar balanced–unbalanced transitions as f. Based on this similar behavior of f and E, one could hypothesize about a possible equivalence between the energy landscape of pairwise interactions, E, and that of triadwise interactions (42), $H := \sum_{(i,j,k)} J_{ij} J_{jk} J_{ki} = f(n_+ + n_-)$. In *SI Appendix*, section M, we at least prove that $E = H(N+1) - H(N)$, where $H(N+1)$ and $H(N)$ are the triple Hamiltonians for systems of size $N+1$ and N, respectively, in the special $G = 1$, $\alpha = 0.5$ case and for fully connected networks.

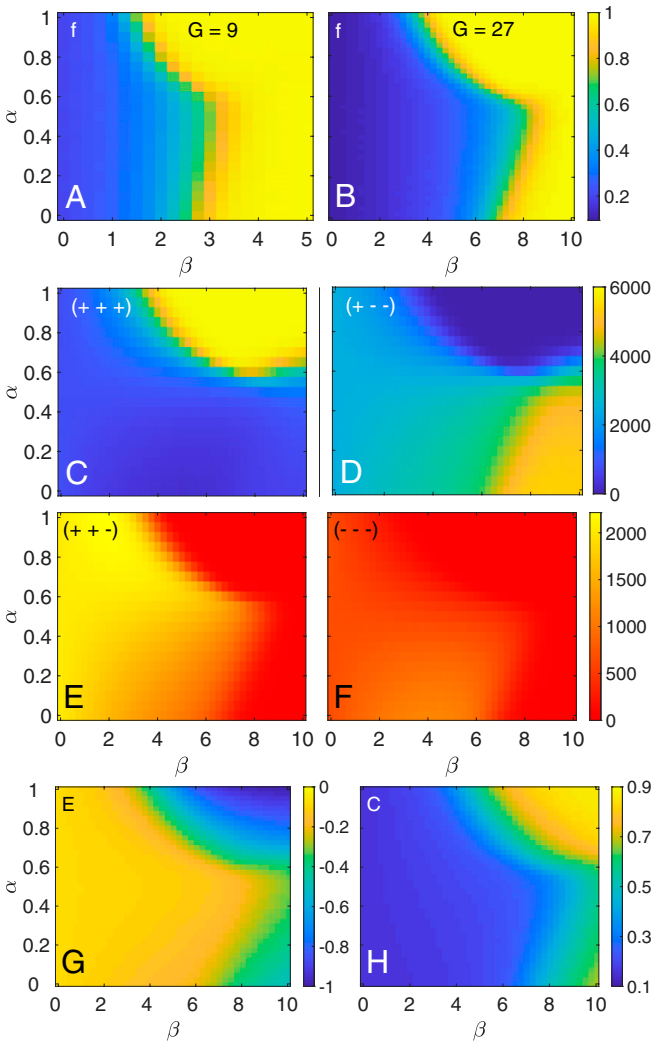

Fig. 2. Phase diagram in the social balance order parameter, *f*, as a function of α and β for individuals with $G = 9$ (*A*) and $G = 27$ (*B*) different opinions they consider for link updates. Social balance (yellow) emerges for a wide range of parameters. Triangle numbers are shown for $(+++)$ in *C*, $(+--)$ in *D*, $(++-)$ in *E*, and $(---)$ in *F*. The two types of social balance appear in different regions (*C* and *D*) in parameter space. Unbalanced triangles (+ + –) only appear for small β values, and (– – –) is marginal in numbers. We present the phase diagrams of the normalized global energy, *E*, in *G* and the average correlation between opinions of an agent with that of its friends, *C*, in *H*. $G = 27$ in *C*–*H*. Results are averaged over 100 runs on regular ring networks with $K = 8$ and $N = 1000$.

Triangle Statistics. The balanced phase (in a steady state) contains different proportions of triads of the types $(+++)$ and $(+--)$. In particular, the state with a majority of $(+++)$ triads can be distinguished from the one consisting of mostly $(+--)$ by comparing n_{Δ_3} with n_{Δ_1}. n_{Δ_ℓ} denotes the number of triads with ℓ positive links. In Fig. 2 *C*–*F*, we show the respective number of triads as a function of α and β and find a dynamical transition between two types of balanced states: one with $n_{\Delta_3} \simeq n_+$ (the yellow region in Fig. 2*C*) and another with $n_{\Delta_1} \simeq 0.9\, n_+$ (the yellow region in Fig. 2*D*). This transition does not affect the numbers of unbalanced triads in Fig. 2 *E* and *F*. From the α dependence of the level of balance and the relative fractions of different triads in Fig. 3 *A* and *B*, respectively, we find that such transition necessarily happens after a critical value α_c is

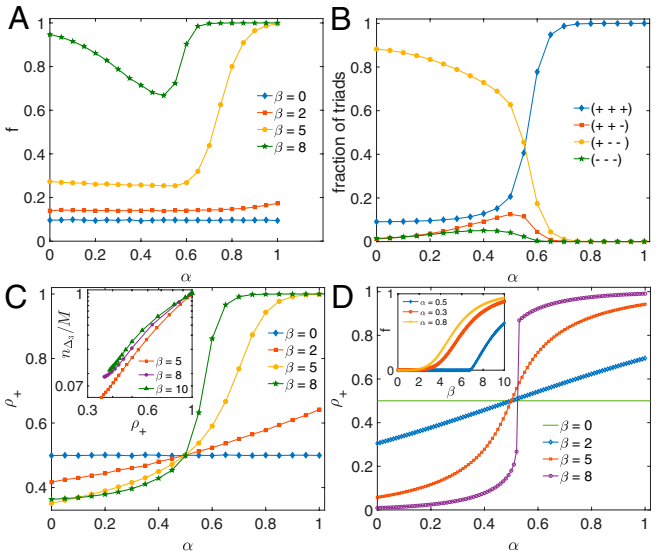

Fig. 3. (*A*) Order parameter, *f*, for $\beta = 0, 2, 5, 8$. (*B*) Fraction of triads of different types for fixed $\beta = 8$. (*C*) Fraction of positive links, ρ_+, in the steady states for various $\beta = 0, 2, 5, 8$ (in the main panel) and fraction of $(+++)$ triads as function of ρ_+ for different β (*Inset*). *Inset* with log–log scale shows that to a good degree, n_{Δ_3}/M can be approximated by ρ_+^3, where $M = n_+ + n_-$ is the total number of triangles. (*D*) Analytical solution for the steady-state values of ρ_+ (in the main panel) and *f* (*Inset*) from Eq. **2** within the uncorrelated link approximation as functions of α and β, respectively. All results from simulations in *A*–*C* are averaged over 100 runs, $K = 8$, $G = 27$, and $N = 1000$.

crossed. There, we observe that the fraction of $(+++)$ triads $(+--)$ continuously increases (decreases) as α increases. Closer inspection suggests that this transition can be associated with the change in the fraction of positive links, ρ_+, with increasing α. In fact, ρ_+ is always a monotonically increasing function of α as seen in Fig. 3*C*. The curves of ρ_+ for various β all intersect at $\alpha = 0.5$, where $\rho_+ = 0.5$. Since links in the model are generally correlated, the number of triads with all positive links, n_{Δ_3}, is not equal to $\rho_+^3(n_+ + n_-)$, which would only be valid for random networks with uncorrelated links. However, in Fig. 3 *C*, *Inset*, we see that $n_{\Delta_3}/(n_+ + n_-)$ is well approximated by ρ_+^3, meaning that it increases with increasing ρ_+ in a similar fashion as for uncorrelated networks. Based on this observation, we present an analytical approach, where we assume that links are uncorrelated. In *SI Appendix*, section D, we show that this approximation leads to the following equations for the stationary values of ρ_+ and f in the limit of $G \to \infty$:

$$\frac{\rho_*}{1-\rho_*} = \exp\left\{-\frac{2\beta K}{G}\left(1-\alpha-\rho_*\right)\right\}, \quad f_* = (2\rho_* - 1)^3 . \qquad [2]$$

Fig. 3*D* shows that while the analytical solutions for ρ_+ are not identical with the numerical values, they reproduce the qualitative α dependence of ρ_+ observed in Fig. 3*C* reasonably well. The analytical approach also yields a qualitative understanding of the unbalanced–balanced phase transition in terms of the order parameter f as shown in Fig. 3 *D*, *Inset*, where f starts to increase from zero above a critical value β_c. More details on the analytical computation are in *SI Appendix*, section D.

In *SI Appendix*, section E, we show the *z* scores for triangle frequencies as a function of α and β on the ring topology (Table 1). The z_i score for triads with *i* positive links is defined as the difference between the observed triangle numbers and that expected from a null model with reshuffling edge signs, normalized by the SD of the latter. A score of 10 means that this difference is 10 times larger than the SD

Table 1. The *z* scores of the triangle statistics of real social networks of the *Pardus* society (first line) in comparison with various model predictions

Social networks	(+ + +)	(+– –)	(+ + –)	(– – –)
Pardus	71	47	–112	–5
Model on ring	[5 48]	[13 71]	[–69 –8]	[–54 8]
Model on *Pardus*	[11 87]	[–9 242]	[–244 –30]	[–69 2]
Optimal (α^*, β^*) *Pardus*	52	46	–99	–8

We show minimal and maximal *z* scores observed in simulations over a wide (α, β) parameter region in brackets for the presented model on a ring network with $K = 8$, $N = 1000$ (second line), and the *Pardus* society topology (third line). The fourth line presents the *z* scores for model simulations on the *Pardus* network at the optimal parameters $(\alpha^*, \beta^*) = (0.8, 0.4)$. We fixed $G = 9$ in all of these computations.

(*SI Appendix*, section E). Table 1 contains the ranges of the z_i scores ([min max] for the covered parameter range of α and β) for the ring topology. z_1 and z_3 are strongly positive, ranging from values of 5 to 71; z_0 and z_2 are negative between –69 and 8. The z_i scores also reflect the different phases (*SI Appendix*, Fig. S5).

Cluster Size Distribution of Positively Linked Groups. We next focus on the size distribution of positive clusters (of friends), where nodes are connected by positive links only. This distribution provides important information about the fragmentation/cohesion of societies (40). A broad distribution of cluster sizes indicates a fragmented structure; for a cohesive society, one would expect a few large clusters of macroscopic size that might percolate the system. Remarkably, we find that the balanced–unbalanced phase transition has a substantial effect on the positive cluster size distribution. Fig. 4*A* shows the size distributions in the balanced phase ($\beta = 3$; orange) on a regular ring topology with $K = 8$. We find a clear exponential decay of cluster sizes with the decay rate $\lambda = -0.0116$. Due to fluctuations in the unbalanced phase, where the system remains active even after very long simulation times, links still undergo many changes, resulting in the appearance of large (and constantly restructuring) clusters. Distributions broaden in the unbalanced phase ($\beta = 1$) (Fig. 4*A*, blue) but remain exponential.

Model Predictions on Real Topologies and Empirical Validation. We now use the model to predict triangle statistics on real social topologies and compare them with the actual situation. To this end, we consider the society of the *Pardus* game, for which we have temporal signed graphs available that contain all friendship and enmity links between the players (5). From these data, we extract the (unsigned) contact network between a subset of 4,232

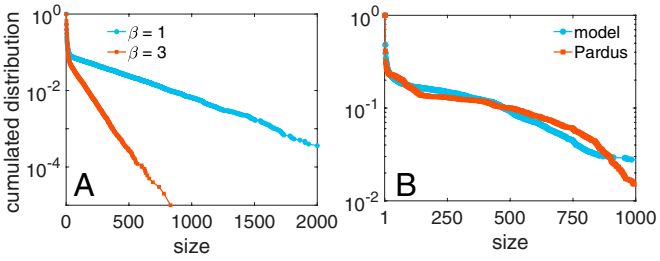

Fig. 4. (*A*) Distribution of cluster sizes of positively linked individuals on a regular ring network with $K = 8$; $\beta = 3$ ($\beta = 1$) corresponds to the balanced (unbalanced) phase. $N = 10,000$, $G = 9$, and $\alpha = 0.5$. We find exponential distributions of the form $P(s) \propto e^{-\lambda s}$ with $\lambda = -0.0116$ for $\beta = 3$ and $\lambda = -0.0027$ for $\beta = 1$. (*B*) Empirical size distribution of clusters detected by the generalized Louvain (60) in the *Pardus* society (orange) and the corresponding model prediction from simulations on a network with the same topology as the *Pardus* society (blue). Results are averaged over 100 simulations for $G = 9$, $\alpha = 0.7$, and $\beta = 0.25$. The *Pardus* data are collected from the last 100 network snapshots (details are in *Materials and Methods*).

active players (*Materials and Methods*) and use its actual topology as an input network for our model. We compute the balance, f; the fraction of positive links, ρ_+; the number of triangles of different types; and the z_i scores. Results are shown in Fig. 5 for a range of α and β and a fixed value, $G = 9$. This value was chosen for practical reasons (reasonable simulation times)—but it is also useful for testing the model's prediction. Our result remains robust with respect to other values of G. It is important to remark that we do not infer the opinions of the game players from the dataset but randomly assign them a value of 1 or -1 in the simulations. We find a similar situation as in Fig. 2 *A* and *B* (i.e., a shifted phase diagram of f in Fig. 5 *A* and *B*), suggesting an effect of a heterogeneous topology on the balanced–unbalanced transition. A dynamical transition in the proportions of $(+++)$ and $(+--)$ triangles also occurs in Fig. 5 *C*–*F*, similarly to what was obtained in Fig. 2 *C*–*F*. The ranges of z_i scores over the covered parameter region are found in Table 1 (third line), and the full computation is shown in Fig. 5 *G*–*J*.

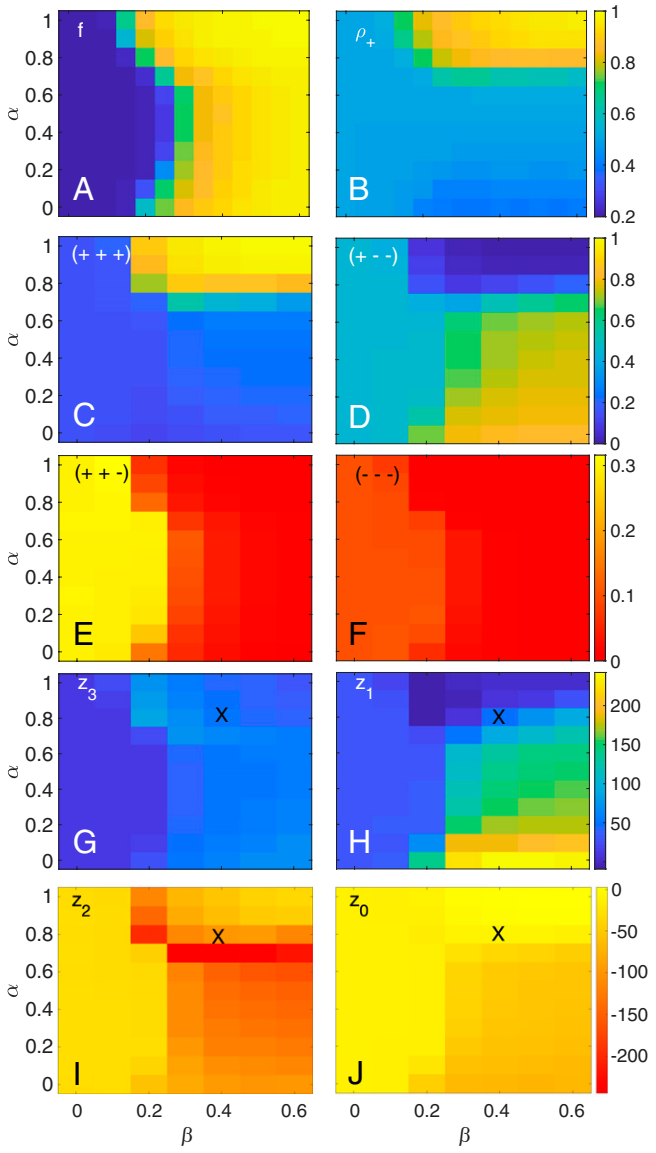

Fig. 5. Model predictions for (*A*) the order parameter, *f*, and (*B*) the fraction of positive links, ρ_+, as functions over a wide parameter region (α, β) on networks whose topology is identical to those in the *Pardus* society. The structure of these phase diagrams is similar to what was obtained for the ring topology. (*C*–*F*) Fractions of different triad types. A transition between two types of balanced states occurs—very similar to the ring topology. (*G*–*J*) The *z* scores of these triads. Results are averaged over 100 independent simulations of the model for $G = 9$. For every simulation, we generate an ensemble of 100 null models with the *Pardus* topology and random link signs, where ρ_+ is fixed to that observed in this simulation. Results are first averaged over this ensemble of null models and then, over the set of simulation runs. The marker X denotes the parameter values $(\alpha^*, \beta^*) = (0.8, 0.4)$ that yield the closest *z* score distance to the real network.

We compute the z scores by using a null model that is generated from reshuffling the links' signs on this simulated network (details are in *SI Appendix*, section E). As for the ring topology, balanced triads have high positive z scores, indicating strong overrepresentation. We also find a wider range of z scores than for the ring topology. Using a procedure of finding the minimal Euclidean distance between the empirical values of the z scores in the actual *Pardus* society and that obtained in the simulated networks, we find the optimal parameters $(\alpha^*, \beta^*) = (0.8, 0.4)$ as the best estimation (*SI Appendix*, section E). The corresponding values of the z_i scores at this point are marked with an "X" in Fig. 5 *G*–*J* and are mentioned in Table 1 (fourth line). Note the similarity to the actual z_i scores of the *Pardus* society (first line).

Next, we compute the clusters in each of the last 100 network snapshots of the actual *Pardus* network with the generalized Louvain algorithm (60) (*SI Appendix*, section F). The empirical cluster size distribution of *Pardus* is compared with that which emerges from the model when running on the *Pardus* society topology. Note a difference between positive clusters and those detected by the generalized Louvain algorithm. The former consists of only positive links, while the latter generally contains a small number of negative links. We show the result in Fig. 4*B*, where without explicit knowledge about the opinions of *Pardus* game players, for simplicity, we chose $G = 9$ and arrive at the values of $\alpha = 0.7$, $\beta = 0.25$ as the point at which the simulation yields f closest to the empirical value $f = 0.69$.

Discussion

Social balance theory is widely believed to be one of the most important mechanisms that lead to structural stability of societies. Here, we offer an alternative explanation of the emergence of balanced triads based on dyadic relations between individuals who establish their relations through a standard homophily-based mechanism. Individuals tend to minimize their own social stress levels by updating opinions and social links on the same timescale. Within a Hamiltonian framework, we find a phase transition from an unbalanced to a balanced regime when decreasing social temperature, $T = \beta^{-1}$. The latter captures the preference for opinion and link updates that lower social stress.

The transition is remarkably robust under changes in the network size and topology. On the ring topology, it exhibits a simple scaling dependence on the average degree, K, and the number of independent opinions, G. This shows that generically balanced situations are expected if individuals attempt to lower their stress in dyadic homophily-based interactions. The robustness of the model makes it immediately applicable to real situations.

Inside the balanced phase, a second transition occurs between two types of steady states, as the parameter, α, controlling the relative weights of positive and negative interactions varies. This explains the dominance of different types of balanced triangles in the balanced phase as a consequence of the importance of friendship to individual stress. A so-called "paradise" society, where only positive links exist, is unreachable unless friendship outweighs enmity in the stress calculation.

Remarkably, we find small parameter regions where the triangle statistics for four triangle types are simultaneously consistent with what is observed in real societies. The probability to obtain such results by pure chance is practically zero. Further, we show that the empirical values of the triangle z scores fall within a range that is predicted by the model. The model also allows us to predict

clusters of predominantly positively linked individuals. While for the regular ring topology, we find exponential distributions, we find more involved functional forms for realistic network topologies. Again, the empirical distribution of cluster sizes follows these predictions to a large extent.

There exist important relations to previous models on social balance emerging from the interplay between homophily and the dynamics of multidimensional opinions (in particular, to refs. 24 and 26). Here, it is important to stress the main idea of the work; we believe that it is generally very hard for individuals to factor in the triadic relations between their social contacts in the process of social tie formation. Even though we believe (even from everyday experience) that triadic information plays a role for very close relationships, it is unrealistic to base general link formation in societies on triadic information due to the amount of information processing that would be necessary. Our simple model thus focuses on dyadic relations only (tendency to be friends with those similar and enemies with those dissimilar) rather than on balancing social triads (as, e.g., in ref. 24). Note that the presented model also uses the same Hebbian learning rule (61) that defines the link weights through a correspondence between the states of its nodes, as in ref. 26. In contrast to their use of a parameter that controls the relative rate of this learning process in the opinion updates, we do not assume such a timescale separation. Coevolution on comparable timescales of social interactions and opinions leads to faster convergence of social balance and to a much reduced probability of getting trapped in partially balanced states, as was observed in ref. 26.

The model is certainly minimalistic in various aspects. It does not consider asymmetries in social relations nor correlations between different dimensions of opinions. It uses only binary relationships derived from binary opinions. An obvious extension to the model would be to consider opinions that are randomly drawn from continuous distributions, $P_i(s^{(l)})$, with $l = 1, 2, \cdots, G$ and to derive weighted (and signed) links by modifying the homophily rule to $J_{ij} = \sum_{l=1}^{G} \int ds^{(l)} P_i(s^{(l)}) P_j(s^{(l)})$, as proposed in ref. 62. The model treats contributions to social relations from opinions on different issues equally, while in reality, topics that might influence the relations between two people are generally not of equal importance. It might happen that people who are similar on many topics still encounter massive tension when they differ on one extremely important topic. This can be captured by defining $J_{ij} = \sum_{l=1}^{G} w_l \int ds^{(l)} P_i(s^{(l)}) P_j(s^{(l)})$, where w_l is the relative weight of the lth opinion dimension. Moreover, the interaction J_{ij} can also depend on the distance between i and j in some (hidden) metric space in which they are embedded. Since such a node embedding can result in a high density of triangles in unsigned graphs (63), it would be interesting to understand how a properly defined underlying geometry can affect the presented results for triad formation in signed graphs. Also, the model has not yet taken into account a set of constraints on the update of one opinion due to the existence of a belief system that could be represented as a network of relations among opinions (64–66). Another simplification is that we restrict ourselves to a fixed base network topology, neglecting the temporal evolution of social network structures (67) [in particular, those that involve triadic closure (68, 69)].

An interesting direction to consider in future work is to generalize the presented framework of dyadic homophilic interactions that explains balanced triad formation to processes of cohesive group formation. In this respect, the good agreement between the empirical distribution of cluster size in *Pardus* and that obtained from the model is much encouraging. It seems feasible to extend the model to a situation of opinion formation processes in groups, where individuals or institutions have a set of opinions or values. It is conceivable that decision—or voting—behavior is influenced by the overlap of these opinion vectors, similar to what we have shown here. In an exploratory exercise, we computed the triad statistics of a network derived from the voting behavior of the United Nations General Assembly that includes the voting patterns of United Nations members in 74 sections from 1946 to 2019 (70). We find z scores close to the range of the model outputs. Details are in *SI Appendix*, section G.

Materials and Methods

Details of Networks from the *Pardus* Dataset. The data of the *Pardus* game contain lists of friendships and enmities of the game players over a period of 1,235 d. Based on these lists, we can construct the temporal network at consecutive time windows as well as study the evolution of triangle numbers and z scores. At the last time point, the network consists of 4,232 nodes, 25,699 negative directed links, and 39,095 positive directed links. We first make these directed links undirected as follows; an undirected unweighted link between two nodes is established whenever there exists at least one directional link between those nodes in the original lists. We then assign 1 (-1) to the links created in the previous step according to the signs of the corresponding (directed) links, and in doing that, we remove all those links whose signs are different from their reversely directed links. The average degree of the obtained network is $K \simeq 24.7$. More details of network characteristics are in refs. 5 and 52.

Additional Order Parameters. We use two additional measures to quantify the transition between balanced and unbalanced phases that would also work for network topologies that do not have triangles, such as trees, bipartite graphs, or square lattices. The pairwise correlation between two connected nodes can always be defined. Since at low temperatures, individuals prefer to reduce their stress by becoming more similar to their friends over time, one would expect that for any agent i, the (normalized) similarity between i and a friend of it j, $\mathbf{s}_i \cdot \mathbf{s}_j/G$, actually increases from a slightly positive value toward one as the system transits from the unbalanced to the balanced phase. We define an average similarity score of an individual with his friends as follows:

$$C = \frac{1}{NG} \sum_{i \in \mathcal{N}^*} \sum_{j: J_{ij}=1} \frac{\mathbf{s}_i \cdot \mathbf{s}_j}{\mathcal{N}_i^+}, \qquad [3]$$

where $\mathcal{N}^*$ denotes the set of nodes of which each has at least one friend, $\mathcal{N}^* := \{i \in \mathcal{V} | \exists j \in \mathcal{V} \text{ with } J_{ij} = 1\}$, and where $\mathcal{N}_i^+$ is the set of friends of i, $\mathcal{N}_i^+ := \{j \in \mathcal{V} | J_{ij} = 1\}$.

Data Availability. Previously published data were used for this work (70). All other data are included in the manuscript and/or *SI Appendix*.

ACKNOWLEDGMENTS. This work was supported in part by Austrian Science Fund Grant P 33751 and by Austrian Science Promotion Agency Project Grant 857136. We thank Mirta Galesic, Henrik Olsson, Johannes Sorger, Fariba Karimi, and Eddie Lee for helpful discussions. We also thank two anonymous reviewers for their excellent comments and suggestions.

1. F. Heider, Attitudes and cognitive organization. *J. Psychol.* **21**, 107–112 (1946).
2. A. G. Greenwald *et al.*, A unified theory of implicit attitudes, stereotypes, self-esteem, and self-concept. *Psychol. Rev.* **109**, 3–25 (2002).
3. S. F. Sampson, "A novitiate in a period of change: An experimental and case study of social relationships," PhD thesis, Cornell University, Ithaca, NY (1968).
4. J. Leskovec, D. Huttenlocher, J. Kleinberg, "Signed networks in social media" in *Proceedings of the SIGCHI Conference on Human Factors in Computing Systems*, G. Fitzpatrick, S. Hudson, K. Edwards, T. Rodden, Eds. (ACM, New York, NY, 2010), pp. 1361–1370.
5. M. Szell, R. Lambiotte, S. Thurner, Multirelational organization of large-scale social networks in an online world. *Proc. Natl. Acad. Sci. U.S.A.* **107**, 13636–13641 (2010).
6. D. Cartwright, F. Harary, Structural balance: A generalization of Heider's theory. *Psychol. Rev.* **63**, 277–293 (1956).
7. F. Harary, On the notion of balance of a signed graph. *Mich. Math. J.* **2**, 143–146 (1953).
8. J. A. Davis, Clustering and structural balance in graphs. *Hum. Relat.* **20**, 181–187 (1967).
9. A. Bramson *et al.*, Understanding polarization: Meanings, measures, and model evaluation. *Philos. Sci.* **84**, 115–159 (2017).
10. G. Facchetti, G. Iacono, C. Altafini, Computing global structural balance in large-scale signed social networks. *Proc. Natl. Acad. Sci. U.S.A.* **108**, 20953–20958 (2011).
11. O. Askarisichani, A. K. Singh, F. Bullo, N. E. Friedkin, The 1995-2018 global evolution of the network of amicable and hostile relations among nation-states. *Commun. Phys.* **3**, 215 (2020).
12. C. Altafini, Consensus problems on networks with antagonistic interactions. *IEEE Trans. Automat. Contr.* **58**, 935–946 (2013).

13. M. Medo, M. S. Mariani, L. Lü, The fragility of opinion formation in a complex world. *Commun. Phys.* **4**, 75 (2021).
14. M. Saeedian, N. Azimi-Tafreshi, G. R. Jafari, J. Kertesz, Epidemic spreading on evolving signed networks. *Phys. Rev. E* **95**, 022314 (2017).
15. H. J. Li, W. Xu, S. Song, W. X. Wang, M. Perc, The dynamics of epidemic spreading on signed networks. *Chaos Solitons Fractals* **151**, 111294 (2021).
16. A. Fontan, C. Altafini, A signed network perspective on the government formation process in parliamentary democracies. *Sci. Rep.* **11**, 5134 (2021).
17. O. Askarisichani *et al.*, Structural balance emerges and explains performance in risky decision-making. *Nat. Commun.* **10**, 2648 (2019).
18. K. Kulakowski, P. Gawronski, P. Gronek, The Heider balance: A continuous approach. *Int. J. Mod. Phys. C* **16**, 707–716 (2005).
19. S. A. Marvel, J. Kleinberg, R. D. Kleinberg, S. H. Strogatz, Continuous-time model of structural balance. *Proc. Natl. Acad. Sci. U.S.A.* **108**, 1771–1776 (2011).
20. V. A. Traag, P. Van Dooren, P. De Leenheer, Dynamical models explaining social balance and evolution of cooperation. *PLoS One* **8**, e60063 (2013).
21. M. J. Krawczyk, K. Kulakowski, Z. Burda, Towards the Heider balance: Cellular automaton with a global neighborhood. *Phys. Rev. E* **104**, 024307 (2021).
22. T. Antal, P. L. Krapivsky, S. Redner, Dynamics of social balance on networks. *Phys. Rev. E Stat. Nonlin. Soft Matter Phys.* **72**, 036121 (2005).
23. T. Antal, P. Krapivsky, S. Redner, Social balance on networks: The dynamics of friendship and enmity. *Physica D* **224**, 130–136 (2006).
24. P. J. Górski, K. Bochenina, J. A. Hołyst, R. M. D'Souza, Homophily based on few attributes can impede structural balance. *Phys. Rev. Lett.* **125**, 078302 (2020).
25. A. Parravano, A. Andina-Díaz, M. A. Meléndez-Jiménez, Bounded confidence under preferential flip: A coupled dynamics of structural balance and opinions. *PLoS One* **11**, e0164323 (2016).
26. M. W. Macy, J. A. Kitts, A. Flache, S. Benard, "Dynamic social network modeling and analysis: Workshop summary and papers" in *Polarization in Dynamic Networks: A Hopfield Model of Emergent Structure*, R. Breiger, K. Carley, P. Pattison, Eds. (The National Academies Press, Washington, DC, 2003), pp. 162–173.
27. I. Agbanusi, J. Bronski, Emergence of balance from a model of social dynamics. *SIAM J. Appl. Math.* **78**, 193–225 (2018).
28. P. Singh, S. Sreenivasan, B. K. Szymanski, G. Korniss, Competing effects of social balance and influence. *Phys. Rev. E* **93**, 042306 (2016).
29. M. Saeedian, M. San Miguel, R. Toral, Absorbing phase transition in the coupled dynamics of node and link states in random networks. *Sci. Rep.* **9**, 9726 (2019).
30. M. Saeedian, M. S. Miguel, R. Toral, Absorbing-state transition in a coevolution model with node and link states in an adaptive network: Network fragmentation transition at criticality. *New J. Phys.* **22**, 113001 (2020).
31. N. P. Hummon, P. Doreian, Some dynamics of social balance processes: Bringing Heider back into balance theory. *Soc. Networks* **25**, 17–49 (2003).
32. Z. Wang, W. Thorngate, Sentiment and social mitosis: Implications of Heider's balance theory. *J. Artif. Soc. Soc. Simul.* **6**, 1–2 (2003).
33. A. V. D. Rijt, The micro-macro link for the theory of structural balance. *J. Math. Sociol.* **35**, 94–113 (2011).
34. P. Abell, M. Ludwig, Structural balance: A dynamic perspective. *J. Math. Sociol.* **33**, 129–155 (2009).
35. R. Singh, S. Dasgupta, S. Sinha, Extreme variability in convergence to structural balance in frustrated dynamical systems. *EPL* **105**, 10003 (2014).
36. A. Kargaran, G. R. Jafari, Heider and coevolutionary balance: From discrete to continuous phase transition. *Phys. Rev. E* **103**, 052302 (2021).
37. R. Shojaei, P. Manshour, A. Montakhab, Phase transition in a network model of social balance with Glauber dynamics. *Phys. Rev. E* **100**, 022303 (2019).
38. P. Manshour, A. Montakhab, Dynamics of social balance on networks: The emergence of multipolar societies. *Phys. Rev. E* **104**, 034303 (2021).
39. F. Rabbani, A. H. Shirazi, G. R. Jafari, Mean-field solution of structural balance dynamics in nonzero temperature. *Phys. Rev. E* **99**, 062302 (2019).
40. T. Minh Pham, I. Kondor, R. Hanel, S. Thurner, The effect of social balance on social fragmentation. *J. R. Soc. Interface* **17**, 20200752 (2020).
41. T. M. Pham, A. C. Alexander, J. Korbel, R. Hanel, S. Thurner, Balance and fragmentation in societies with homophily and social balance. *Sci. Rep.* **11**, 17188 (2021).
42. S. A. Marvel, S. H. Strogatz, J. M. Kleinberg, Energy landscape of social balance. *Phys. Rev. Lett.* **103**, 198701 (2009).
43. A. M. Belaza *et al.*, Statistical physics of balance theory. *PLoS One* **12**, e0183696 (2017).
44. A. M. Belaza *et al.*, Social stability and extended social balance—quantifying the role of inactive links in social networks. *Physica A* **518**, 270–284 (2019).
45. P. F. Lazarsfeld, R. K. Merton, *Freedom and Control in Modern Society*, M. Berger, T. Abel, C. H. Page, Eds. (Van Nostrand, 1954), pp. 18–66.
46. M. McPherson, L. Smith-Lovin, J. M. Cook, Birds of a feather: Homophily in social networks. *Annu. Rev. Sociol.* **27**, 415–444 (2001).
47. P. Block, T. Grund, Multidimensional homophily in friendship networks. *Netw Sci (Camb Univ Press)* **2**, 189–212 (2014).
48. I. Smirnov, S. Thurner, Formation of homophily in academic performance: Students change their friends rather than performance. *PLoS One* **12**, e0183473 (2017).
49. A. Flache, M. W. Macy, Small worlds and cultural polarization. *J. Math. Sociol.* **35**, 146–176 (2011).
50. R. Axelrod, J. J. Daymude, S. Forrest, Preventing extreme polarization of political attitudes. *Proc. Natl. Acad. Sci. U.S.A.* **118**, e2102139118 (2021).
51. F. Jordán, Children in time: Community organization in social and ecological systems. *Curr. Sci.* **97**, 1579–1585 (2009).
52. M. Szell, S. Thurner, Measuring social dynamics in a massive multiplayer online game. *Soc. Networks* **32**, 313–329 (2010).
53. M. Szell, S. Thurner, Social dynamics in a large-scale online game. *Adv. Complex Syst.* **15**, 1250064 (2012).
54. M. Mezard, G. Parisi, M. Virasoro, *Spin Glass Theory and Beyond* (World Scientific, 1986).
55. R. J. Baxter, *Exactly Solved Models in Statistical Mechanics* (Elsevier, 2016).
56. E. Estrada, M. Benzi, Walk-based measure of balance in signed networks: Detecting lack of balance in social networks. *Phys. Rev. E Stat. Nonlin. Soft Matter Phys.* **90**, 042802 (2014).
57. A. Kirkley, G. T. Cantwell, M. E. J. Newman, Balance in signed networks. *Phys. Rev. E* **99**, 012320 (2019).
58. P. Abell, Structural balance in dynamic structures. *Sociology* **2**, 333–352 (1968).
59. D. J. Watts, S. H. Strogatz, Collective dynamics of 'small-world' networks. *Nature* **393**, 440–442 (1998).
60. M. Rubinov, O. Sporns, Weight-conserving characterization of complex functional brain networks. *Neuroimage* **56**, 2068–2079 (2011).
61. D. Hebb, *The Organization of Behavior: A Neuropsychological Theory* (Wiley, 1949).
62. M. J. Palazzi *et al.*, An ecological approach to structural flexibility in online communication systems. *Nat. Commun.* **12**, 1941 (2021).
63. D. Krioukov, Clustering implies geometry in networks. *Phys. Rev. Lett.* **116**, 208302 (2016).
64. N. Rodriguez, J. Bollen, Y. Y. Ahn, Collective dynamics of belief evolution under cognitive coherence and social conformity. *PLoS One* **11**, e0165910 (2016).
65. N. E. Friedkin, A. V. Proskurnikov, R. Tempo, S. E. Parsegov, Network science on belief system dynamics under logic constraints. *Science* **354**, 321–326 (2016).
66. C. M. Rawlings, Cognitive authority and the constraint of attitude change in groups. *Am. Sociol. Rev.* **85**, 992–1021 (2020).
67. G. Kossinets, D. J. Watts, Empirical analysis of an evolving social network. *Science* **311**, 88–90 (2006).
68. M. E. J. Newman, Clustering and preferential attachment in growing networks. *Phys. Rev. E Stat. Nonlin. Soft Matter Phys.* **64**, 025102 (2001).
69. U. Bhat, P. L. Krapivsky, S. Redner, Emergence of clustering in an acquaintance model without homophily. *J. Stat. Mech.* **2014**, 11035 (2014).
70. M. A. Bailey, A. Strezhnev, E. Voeten, Estimating dynamic state preferences from United Nations voting data. *J. Conflict Resolut.* **61**, 430–456 (2017).